

Synthesis and evaluation of a F-labeled triazinediamine analogue for imaging mutant IDH1 expression in gliomas by PET

Satish K Chitneni, Hai Yan, and Michael R. Zalutsky

ACS Med. Chem. Lett., **Just Accepted Manuscript** • DOI: 10.1021/acsmchemlett.7b00478 • Publication Date (Web): 01 May 2018Downloaded from <http://pubs.acs.org> on May 2, 2018

Just Accepted

“Just Accepted” manuscripts have been peer-reviewed and accepted for publication. They are posted online prior to technical editing, formatting for publication and author proofing. The American Chemical Society provides “Just Accepted” as a service to the research community to expedite the dissemination of scientific material as soon as possible after acceptance. “Just Accepted” manuscripts appear in full in PDF format accompanied by an HTML abstract. “Just Accepted” manuscripts have been fully peer reviewed, but should not be considered the official version of record. They are citable by the Digital Object Identifier (DOI®). “Just Accepted” is an optional service offered to authors. Therefore, the “Just Accepted” Web site may not include all articles that will be published in the journal. After a manuscript is technically edited and formatted, it will be removed from the “Just Accepted” Web site and published as an ASAP article. Note that technical editing may introduce minor changes to the manuscript text and/or graphics which could affect content, and all legal disclaimers and ethical guidelines that apply to the journal pertain. ACS cannot be held responsible for errors or consequences arising from the use of information contained in these “Just Accepted” manuscripts.

Synthesis and evaluation of a ^{18}F -labeled triazinediamine analogue for imaging mutant IDH1 expression in gliomas by PET

Satish K. Chitneni^{1*}, Hai Yan², Michael R. Zalutsky^{1,2}

¹Department of Radiology, Duke University Medical Center, Durham, NC 27710, USA. ²Department of Pathology, Duke University Medical Center, Durham, NC 27710, USA

KEYWORDS: IDH mutation, glioma, mutant IDH1 inhibitor, PET imaging, fluorine-18.

ABSTRACT: Mutations in the isocitrate dehydrogenase gene 1 (IDH1) are common in gliomas. Studies suggest that IDH1 mutations are early events in glioma formation and are important drivers of malignant progression. Herein, we report the synthesis and evaluation of a ^{18}F -labeled triazinediamine analogue, [^{18}F]1, as a candidate radiotracer for noninvasive imaging of IDH1 mutations in gliomas by positron emission tomography (PET). *In vitro* studies revealed good binding inhibition potency and binding affinity for [^{18}F]1 in IDH1 mutant glioma cell lines, with a half-maximal inhibitory concentration value (IC_{50}) of 54 nM and an equilibrium dissociation constant (K_d) of 40 nM. *In vivo* studies using mutant IDH1 glioma xenografts showed good tumor uptake of [^{18}F]1 and specific inhibition by the unlabeled 1, but also elevated radioactivity uptake in the bone, suggesting significant defluorination. The results support further optimization of the triazinediamine scaffold to develop a more stable and potent ^{18}F -labeled analogue for PET imaging of IDH1 mutations in gliomas.

Isocitrate dehydrogenase 1 and 2 (IDH1/2) are metabolic enzymes that play key roles in energy production and in maintaining normal redox status in cells. IDH1 exists as a homodimer in the cytosol and in peroxisomes, whereas IDH2 is localized in the mitochondria. IDH1/2 catalyze the reversible conversion of isocitrate to alpha-ketoglutarate (α -KG) with simultaneous generation of NADPH.¹ Mutations in the IDH1 gene and to a lesser extent IDH2 are found in >70% of WHO grades II and III gliomas and in secondary glioblastomas (sGBM).² In most cases, the mutation involves a substitution of arginine-132 with histidine (R132H) in the catalytic site of IDH1, although other amino acid substitutions are also observed in some cases (e.g., R132C, R132S, and R132G).² The most common IDH2 mutation in glioma is R172K, accounting for about 2.5% of all IDH mutations in gliomas. IDH1 and IDH2 mutations are mutually exclusive and result in decreased affinity for isocitrate. However, they also yield a new function that enables the mutant IDH1/2 to reduce α -KG to D-2-hydroxyglutarate (D-2-HG).³ Thus, IDH1/2 mutant gliomas have ~100-fold higher levels of D-2-HG compared to those in wild-type IDH gliomas or the normal brain.³ Studies suggest that D-2-HG functions as an oncometabolite by competitively inhibiting several dioxygenase enzymes that are normally dependent on α -KG as a substrate for their enzymatic activity. Inhibition of these enzymes leads to a genome-wide changes in DNA methylation, trimethylation of histone lysine residues, and induces a block in cellular differentiation.^{4,5} IDH1 mutations have a significant impact also on the levels of several small-molecule biochemicals such as glutamine, glutamate and glutathione metabolites, suggesting that widespread metabolic changes can occur in IDH1 mutant gliomas.⁶

Clinically, patients with IDH1/2 mutant gliomas have better survival compared to patients with wild-type IDH (WT-IDH)

gliomas. The median survival in patients with IDH1/2 mutant glioblastoma or anaplastic astrocytoma is 2-3 times longer than that for patients with WT-IDH tumors from the same histological class.² Recent studies also suggest that IDH1 mutant gliomas may be more sensitive to certain targeted-therapies, and are amenable to maximal surgical resection, supporting the potential usefulness of IDH1 mutation status as a predictive biomarker in addition to its prognostic value.^{7,8} Furthermore, The Cancer Genome Atlas (TCGA) Research Network data have shown that IDH mutation status (mutation in IDH1 or IDH2) along with 1p/19q codeletion status is a more robust biomarker for stratification of clinical risk than outcome predictions based on histologic classification in WHO grades II and III gliomas.⁹ Hence, there is a strong rationale for development of noninvasive imaging methods for IDH1/2 mutations in gliomas. To this end, magnetic resonance spectroscopy (MRS) has been shown to be a valuable tool for noninvasive assessment of D-2-HG as a surrogate marker for IDH1/2 mutations in glioma.¹⁰ The goal of our work was to develop a radiotracer for imaging the expression of mutant IDH1 in gliomas by positron emission tomography (PET). Herein, we present data on radiolabeling and preliminary assessment of a ^{18}F -labeled triazinediamine analogue as a potential radiotracer for PET imaging of the most commonly occurring IDH1 mutation in gliomas, IDH1-R132H.

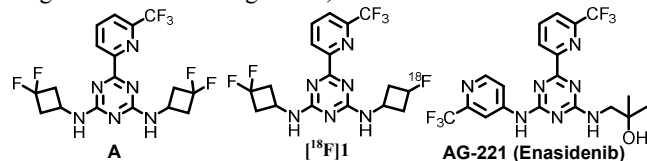
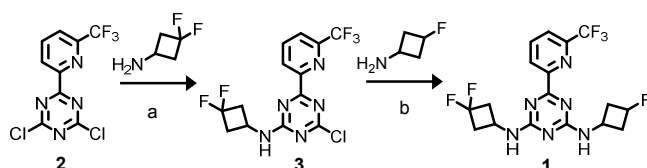


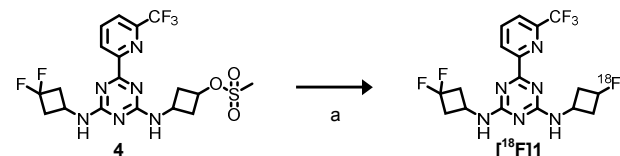
Chart 1. Chemical structures of the reference mutant IDH1 inhibitor A, its ^{18}F -labeled analogue, [^{18}F]1, synthesized in this work, and the FDA-approved mutant IDH2 inhibitor AG-221.

Chart 1 shows the chemical structures of the reference mutant IDH1 inhibitor **A**, its fluorine-18 ($t_{1/2}$: 110 min) labeled analogue [^{18}F]**1** synthesized in this work, and the structurally related AG-221 drug (Enasidenib) that has been approved recently by the FDA for the treatment of relapsed or refractory acute myeloid leukemia (AML) with an IDH2 mutation.¹¹ In the current work, compound **A** was selected as the lead compound for radiolabeling based on its high affinity for mutant IDH1, with a reported half-maximal inhibitory concentration (IC_{50}) value of <50 nM against the clinically-relevant heterozygous mutation, IDH1-R132H/WT.¹² Additionally, it has a near optimal lipophilicity, indicated by its cLogP of 1.9, which is in the desired range for passive diffusion of small-molecules through both cell membranes and the blood-brain-barrier (BBB). In order to facilitate successful incorporation of [^{18}F]fluorine into the molecule by a standard nucleophilic substitution reaction on a methanesulfonate precursor, we opted to synthesize a monofluorocyclobutyl analogue, wherein one of the bis-fluorocyclobutyl substituents in **A** was replaced with a mono-fluorocyclobutyl moiety in **1** (**Scheme 1**).



Scheme 1. Synthesis scheme for the nonradioactive **1**. Reaction conditions: (a) NaHCO_3 , THF, reflux, 7 h; (b) NaHCO_3 , THF, reflux, 3 h.

The synthesis of the unlabeled compound **1** was achieved by a 3-step synthesis procedure reported for **A** and its analogues.¹² The synthesis started with the commercially available 6-(6-(trifluoromethyl)pyridin-2-yl)-1,3,5-triazine-2,4(1*H*,3*H*)-dione, which was first converted to the bischloro derivative **2** by reaction with phosphorous pentachloride in phosphorus oxychloride under reflux conditions. Substitution of the chlorines in **2** with 3,3-difluorocyclobutan-1-amine and 3-fluorocyclobutanamine (*cis/trans* mixture) in sequential reactions in the presence of sodium bicarbonate in THF yielded compound **1** with an overall yield of 18% (**Scheme 1**). The synthesis of the methanesulfonate derivative **4** for radiolabeling was accomplished by using a hydroxy precursor, which was prepared from the monochloro intermediate **3** and 3-aminocyclobutanol similar to that for **1**. Fluorine-18 labeling of **1** was achieved by nucleophilic radiofluorination reaction on the methanesulfonate precursor **4** in a decay-corrected radiochemical yield of $6.3 \pm 1.6\%$ ($n=12$) (**Scheme 2**). The product [^{18}F]**1** was obtained as *cis/trans* mixture and was used as such for all experiments. The lipophilicity of [^{18}F]**1** was evaluated by the shake-flask method,¹³ which revealed a log partition coefficient value (LogP) of 2.2 ± 0.0 ($n=6$) for [^{18}F]**1**.



Scheme 2. Synthesis scheme for [^{18}F]**1**. Reaction conditions: (a) [^{18}F]KF, Kryptofix 222, DMF, 120 °C, 15 min.

The ability of [^{18}F]**1** to bind to IDH1 mutant glioma cells was evaluated using human oligodendroglioma (HOG) cells that were genetically engineered to express IDH1-R132H or WT-IDH1 as described previously.⁶ For the uptake studies,

mutant IDH1 and WT-IDH1 HOG cells cultured in standard 24-well plates were incubated with 18.5 kBq of [^{18}F]**1** for 15–120 min. In these studies, the uptake of [^{18}F]**1** in the mutant IDH1 cell line was about 7.8-fold higher than that in the WT-IDH1 cell line at 15 min, with an uptake of $72.2 \pm 5.5\%$ per mg protein vs. $9.3 \pm 0.4\%$ per mg protein for the WT-IDH1 cell line ($P < 0.0001$). The uptake and the uptake ratios remained high at subsequent time points also (**Figure 1A**). Co-incubation of cells with excess of unlabeled **1** (50 μM) inhibited the uptake of [^{18}F]**1** in the mutant IDH1 cell line by >95% at all time points, confirming the specificity of [^{18}F]**1** uptake (**Figure 1A**). Blocking with the cold compound also inhibited the uptake seen in the WT-IDH1 cell line to a lesser degree, suggesting some displaceable binding on the WT-IDH1 cells.

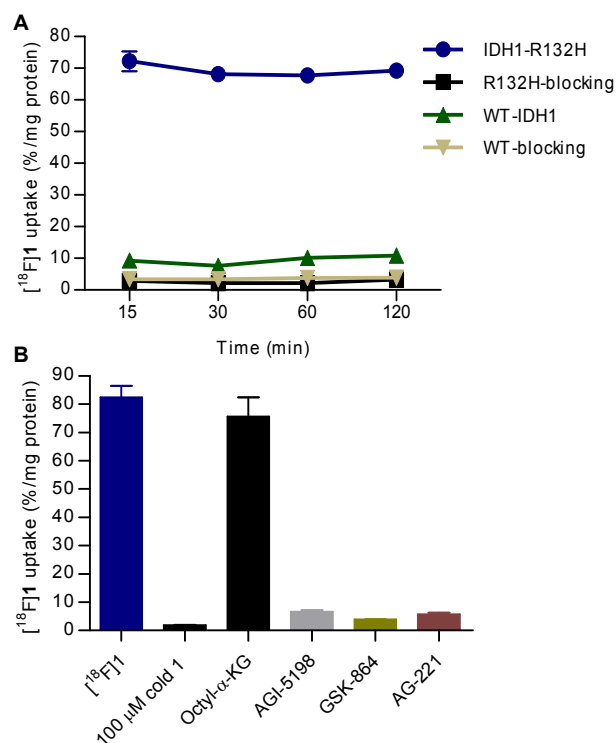


Figure 1. (A). Uptake of [^{18}F]**1** in isogenic human oligodendroglioma cell lines expressing IDH1-R132H or WT-IDH1. Blocking studies were performed by co-incubation with the nonradioactive **1** (50 μM). (B). Blocking studies using known inhibitors of the mutant IDH1/2 and the cell-permeable mutant IDH1 substrate, octyl- α -ketoglutarate. Cells were incubated with [^{18}F]**1** alone or in the presence of the corresponding nonradioactive analogue (100 μM) for 30 min. Data is shown as mean \pm SEM ($n=3-4$).

In order to evaluate the mode of binding of the labeled inhibitor on IDH1 mutant glioma cells, blocking studies were conducted using known inhibitors of the mutant IDH1 (AGI-5198 and GSK-864), mutant IDH2 (AG-221), or octyl- α -KG, which is a cell-permeable analogue of the mutant IDH1 substrate α -KG, all at 100 μM (chemical structures shown in **Figure S1**; Supplementary Information).^{8, 11, 14, 15} In these studies, co-incubation with AGI-5198, GSK-864 and AG-221 resulted in significant inhibition of the [^{18}F]**1** uptake ($P < 0.001$), but octyl- α -KG did not show any significant effect ($P = 0.43$) (**Figure 1B**). These results suggest that AGI-5198, GSK-864 and AG-221 interact with the same binding pocket as **1** on mutant IDH1 or competitively inhibit [^{18}F]**1** binding to mutant IDH1 by some other mechanism. While AGI-5198 and GSK-864 are structurally unrelated to [^{18}F]**1**, AG-221 belongs to the

same chemical class (triazinediamine) and has high selectivity for mutant IDH2 (IC_{50} of 0.1-0.3 μM) vs. mutant IDH1 (IC_{50} of 77.6 μM).¹¹ However, the 100 μM concentration used in blocking studies with AG-221 in the present study is above its IC_{50} for the mutant IDH1 (77.6 μM), and resulted in a 93% inhibition in [^{18}F]1 uptake by the mutant IDH1 cells. Lack of competitive inhibition of [^{18}F]1 by octyl- α -KG suggests that the labeled inhibitor does not compete with the mutant IDH1 substrate α -ketoglutarate for binding to the enzyme, which is consistent with the recently reported data for the AG-221 showing that the mode of binding of the triazinediamine-based inhibitors to the mutant IDH enzyme is non-competitive with respect to the substrate α -KG.¹¹

The inhibitory potency of the nonradioactive **1** against mutant IDH1 was evaluated in competitive inhibition assays using [^{18}F]1 and the HOG-IDH1-R132H cell line. Cells were incubated with [^{18}F]1 and increasing concentrations ($n=8$; 1.4 nM – 3 μM) of nonradioactive **1** under standard cell culture conditions for 1 h. **Figure 2A** shows the inhibitory curve for [^{18}F]1 as a function of increasing concentration of unlabeled **1** in the incubation medium. These studies revealed a binding inhibitory potency (IC_{50}) of 54 nM for **1**, which compares favorably with the reported IC_{50} value of <50 nM for the reference bis-fluoro derivative **A**. We note that a fluorescence-based enzymatic assay was used to determine the IC_{50} of **A** in the literature compared to the radioligand- and cell-based assay used in the current study.¹² In addition, a direct comparison of the inhibitory potency of pure *cis*- and *trans*- isomers of **1** synthesized by using *cis*-3-fluorocyclobutanamine and *trans*-3-fluorocyclobutanamine similar to that shown in **Scheme 1**, revealed somewhat higher inhibitory potency for the *trans* isomer of **1** compared to the *cis* derivative (IC_{50} of 31 nM vs. 55 nM for *cis*-**1**; **Figure 2B**).

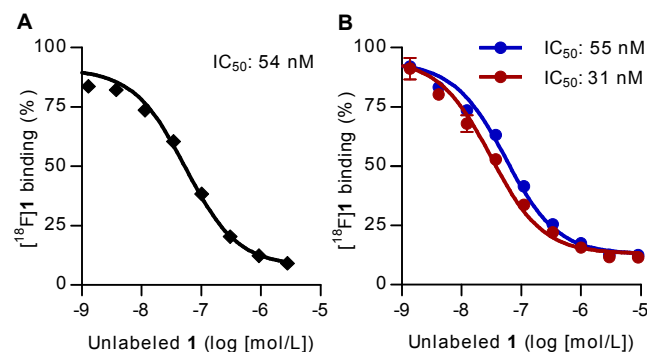


Figure 2. (A). Determination of binding inhibitory potency (IC_{50}) of **1** in competition with [^{18}F]1 in IDH1-R132H mutant HOG cell line. (B) Competitive inhibition curves for pure *cis*- (blue) and *trans*- (red) isomers of **1** in the same cell line. Results are presented as mean \pm SEM ($n=3$).

In order to assess the uptake and binding of [^{18}F]1 in clinically relevant mutant IDH1 tumor models, cell uptake studies also were conducted using a patient-derived IDH1 mutant astrocytoma cell line (IMA) that carried a heterozygous IDH1-R132H/WT mutation as described previously.¹⁶ **Figure 3A** shows an uptake of $18.9 \pm 2.2\%$ of [^{18}F]1 per mg protein after a 1 h incubation in this cell line. Similar to its behavior on the HOG cell line, the uptake could be inhibited significantly by blocking with the unlabeled analogue **1** (50 μM) in parallel experiments. Furthermore, knockout of the R132H allele in the afore-mentioned IMA cell line using CRISPR/Cas-9 gene editing technology (R132H-KO) resulted in a significant decrease in the uptake of [^{18}F]1 ($\sim 55\%$; $P < 0.01$), confirming

the IDH1-R132H mutant specificity of [^{18}F]1 binding to the IMA cell line. Blocking with unlabeled compound **1** decreased uptake in the R132H-KO cell line down to the background radioactivity levels seen in the R132H mutant IMA cell line after blocking (**Figure 3A**), suggesting some displaceable binding in the knockout cell model as well.

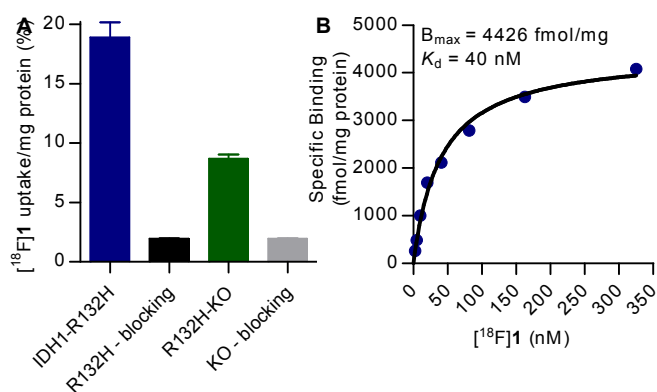


Figure 3. (A). Uptake of [^{18}F]1 in IDH1 mutant anaplastic astrocytoma cell line (IDH1-R132H), and in the IDH1-R132H knockout cell line (R132H-KO). Blocking studies were conducted using 50 μM **1**. (B). Saturation binding curve for the [^{18}F]1 in the IDH1-R132H mutant IMA cell line. Non-specific binding was determined at 50 μM **1**. Experiments were conducted in triplicate, and the data in **Figure 3A** is presented as mean \pm SEM.

Next, saturation binding assays were conducted to determine the binding affinity and the maximal binding capacity (B_{max}) of [^{18}F]1 in the IMA cell line (R132H) (**Figure 3B**). For these experiments, IMA cells were incubated with increasing concentrations of [^{18}F]1 ($n=8$; 2.5 – 325 nM) and binding parameters were determined 1 h after incubation. The equilibrium dissociation constant (K_d) and B_{max} of [^{18}F]1 determined from these assays were 40 nM and 4426 fmol per mg protein, respectively, yielding a B_{max}/K_d ratio of about 110 *in vitro*.¹⁷ Based on the higher inhibitory potency (IC_{50}) of the *trans* isomer compared to the *cis* isomer (**Figure 2B**), we also synthesized the radioactive *trans* isomer (*trans*-[^{18}F]1) by using a *cis* precursor (sulfonate), and as described for [^{18}F]1 in the Supplementary Information. The binding affinity of *trans*-[^{18}F]1 ($K_d = 44$ nM) determined on the IMA cell line was similar to that for non-stereospecific [^{18}F]1, indicating no additional advantage for the radiolabeled *trans*-isomer in terms of binding affinity for mutant IDH1 (**Figure S5**). However, it is worth noting the differences between inhibition potency assays and the binding affinity studies with regard to cell lines, inhibitor concentrations, and possibly mutant IDH1 levels.

The tissue distribution characteristics and tumor uptake properties of [^{18}F]1 were studied in NOD *scid* gamma (NSG) mice bearing HOG-IDH1-R132H tumor xenografts implanted in the flank region. To evaluate uptake specificity in a blocking study, an additional group of animals received unlabeled analogue **1** by intraperitoneal injection (25 mg/kg body weight) 30 min before injection of the radiotracer. **Table 1** shows standardized uptake values (SUVs) for different organs and tissues at 0.5, 1 and 2 h after injection of [^{18}F]1. [^{18}F]1 exhibited rapid clearance from the blood, with a mean SUV of 0.4 ± 0.1 in the blood at 0.5 h, decreasing to 0.1 ± 0.0 at 2 h. In line with its lipophilicity ($\text{Log}P$: 2.15), the labeled compound was eliminated primarily by the hepatobiliary system, with about 25% of the injected dose present in the intestines at 2 h. Based on its high and prolonged radioactivity uptake in the

bone (SUV of 2.3 ± 0.4 at 0.5 h and 2.8 ± 0.5 at 2 h in tibia), [^{18}F]1 appears to undergo significant defluorination *in vivo*. The uptake of [^{18}F]1 in tumor was highest 30 min after injection, with SUV 1.0 ± 0.2 , and decreased at subsequent time points to 0.8 ± 0.2 at 1 h and 0.4 ± 0.2 at 2 h. Pretreatment of animals with unlabeled analogue 1 decreased the uptake of [^{18}F]1 in the tumor significantly, with radioactivity SUV 0.5 ± 0.0 in the blocking group vs. 0.8 ± 0.2 for the unblocked group at 1 h post injection ($P < 0.001$). Calculation of tumor-to-background ratios showed that [^{18}F]1 uptake in tumor was about 2.4-fold higher than that for the muscle, and 8.5-fold higher than that for the whole brain at 30 min. Blocking with the unlabeled compound 1 led to a significant decrease also in tumor-to-background ratios, consistent with competitive inhibition of [^{18}F]1 binding in the tumor by the unlabeled 1 (Table 1).

Table 1. Whole body biodistribution data for [^{18}F]1 in NSG mice bearing IDH1-R132H mutant glioma xenografts (HOG). Data is presented as standard uptake values and as mean \pm SD for 4 animals in each group, except for 1 h (n=9). Tumor-to-background ratios are shown for selected tissues and the blood.

Organ	0.5 h	1 h	1 h - blocking	2 h
Liver	1.2 \pm 0.1	1.4 \pm 0.4	0.9 \pm 0.2*	0.6 \pm 0.1
Spleen	0.4 \pm 0.1	0.3 \pm 0.1	0.4 \pm 0.1*	0.1 \pm 0.0
Lungs	0.6 \pm 0.3	0.6 \pm 0.3	0.7 \pm 0.4	0.3 \pm 0.2
Heart	0.6 \pm 0.1	0.4 \pm 0.1	0.6 \pm 0.1*	0.3 \pm 0.1
Kidneys	0.9 \pm 0.1	0.9 \pm 0.2	1.1 \pm 0.2	0.3 \pm 0.1
Bladder	1.4 \pm 1.0	0.6 \pm 0.4	0.7 \pm 0.2	0.3 \pm 0.1
Stomach	1.3 \pm 0.4	0.8 \pm 0.3	0.8 \pm 0.2	0.4 \pm 0.1
Small intestines	2.2 \pm 0.7	4.6 \pm 1.1	1.1 \pm 0.1*	2.6 \pm 0.8
Large intestines	0.5 \pm 0.1	0.4 \pm 0.1	0.5 \pm 0.1	1.6 \pm 1.5
Bone (tibia)	2.3 \pm 0.4	1.9 \pm 0.5	2.1 \pm 0.2	2.8 \pm 0.5
Muscle	0.4 \pm 0.0	0.4 \pm 0.1	0.7 \pm 0.2	0.2 \pm 0.1
Blood	0.4 \pm 0.1	0.3 \pm 0.1	0.4 \pm 0.0*	0.1 \pm 0.0
Brain	0.1 \pm 0.0	0.1 \pm 0.0	0.2 \pm 0.0*	0.1 \pm 0.0
Tumor	1.0 \pm 0.2	0.8 \pm 0.2	0.5 \pm 0.0*	0.4 \pm 0.2
Tumor/muscle	2.4 \pm 0.6	1.8 \pm 0.3	0.8 \pm 0.3*	2.0 \pm 0.7
Tumor/blood	2.3 \pm 0.1	2.8 \pm 0.4	1.3 \pm 0.1*	2.7 \pm 0.8
Tumor/brain	8.5 \pm 0.9	6.6 \pm 1.0	2.8 \pm 0.4*	5.9 \pm 1.5

*Significant difference compared to the 1 h group

Preliminary microPET imaging studies were conducted in NSG mice bearing HOG-IDH1-R132H tumor xenografts to further evaluate the uptake of [^{18}F]1 in tumor and normal tissues, and to assess the feasibility of imaging mutant IDH1 with PET *in vivo*. Dynamic images were acquired for up to 90 min after injection of [^{18}F]1 at baseline (n=2) or after pretreatment with unlabeled analogue 1 (n=2; 25 mg/kg) given by intraperitoneal injection 30 min before the radiotracer injection (n=2). Time-activity curves (TACs) showing the uptake and clearance of [^{18}F]1 from the mutant IDH1 tumor (HOG) and muscle for a baseline PET scan and blocked animal are shown in Figure 4. Representative microPET images of animals from these groups are also shown next to the corresponding TACs. Comparison of the TACs for the tumor and muscle showed a significantly higher uptake and retention of [^{18}F]1 in the tumor for the baseline PET scan (Figure 4A). [^{18}F]1 showed a peak SUV of ~ 0.7 at 25 min, which decreased slightly at later time points to 0.6 at the end of the 85-min imaging session. Pretreatment of animals with the unlabeled 1 (25 mg/kg) decreased [^{18}F]1 uptake in the tumor significantly, with SUV reaching a maximum of 0.3 for the blocked animal vs. ~ 0.7 for the baseline PET scan. Comparison of TACs for

normal tissues (e.g., muscle, brain) for the two animals indicated slower clearance of [^{18}F]1 from normal tissues in the pretreated animal (e.g., normal brain SUV of 0.3 vs. 0.1 for the untreated animal at 85 min), suggesting possible changes in pharmacokinetics of [^{18}F]1 in the presence of excess of unlabeled 1 used for blocking purposes *in vivo* (25 mg/kg). Consistent with the *ex vivo* tissue distribution data, microPET images also showed significant radioactivity in the liver and intestines at 1 h, reflecting physiological clearance of the labeled compound by the hepatobiliary system. In addition, high uptake of radioactivity in the bone was observed, suggesting that extensive defluorination of [^{18}F]1 occurred *in vivo*.

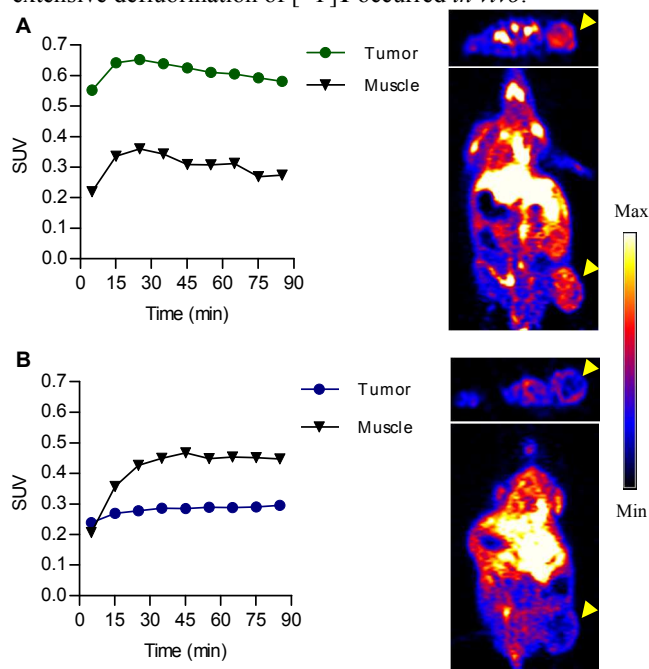


Figure 4. Small animal PET imaging of IDH1 mutant glioma xenografts with [^{18}F]1. Time activity curves for tumor and muscle for mice injected with [^{18}F]1 at baseline (A) or after blocking with nonradioactive 1 (25 mg/kg; i.p.) 30 min before [^{18}F]1 injection (B). PET images of the corresponding animals are shown next to the TACs, for the 25 min time frame. Upper panels in the images show axial view and lower panels show coronal view of the animals. Arrowhead indicates tumors.

In view of their gain-of-function leading to the production of the onco-metabolite D-2-HG, inhibition of mutant IDH1 and IDH2 with small molecules has emerged as a promising therapeutic strategy for targeting IDH1/2 mutations in cancers. This approach has shown rapid progress and led to the successful development and approval of AG-221 (Enasidenib) for the treatment of adult relapsed or refractory AML patients with an IDH2 mutation.¹⁸ Clinical trials of multiple mutant IDH1 inhibitors representing a variety of chemical scaffolds are also ongoing. Of these, AG-120 (Ivosidenib) is in the most advanced stage of investigation and is currently being evaluated in phase I-III clinical trials in multiple cancer types including glioma (clinicaltrials.gov). Biochemical and mechanistic studies have shown that these inhibitors bind to and inhibit the mutant IDH1 enzyme through different mechanisms. For example, compounds based on a phenyl-glycine scaffold (e.g. AGI-5198) inhibit mutant IDH1 by competitive inhibition with respect to the substrate α -KG.^{14, 19} A recent report suggests that they also may bind to an allosteric magnesium binding pocket at the dimer interface and inhibit mutant IDH1 in competition with Mg^{2+} .²⁰ In this regard, triazinediamine ana-

logues such as **1** potentially offer a significant advantage for radiotracer development because they do not have to compete with the endogenous substrate α -KG or NADPH for binding.¹¹ With the goal of developing radiolabeled compounds for imaging mutant IDH1, we previously synthesized and evaluated fluorine-18 and radioiodinated analogues based on a benzenesulfonamide scaffold, which has been used in the past for developing small molecule mutant IDH1 inhibitors.²¹ Compared to these labeled benzenesulfonamide analogues, [¹⁸F]**1** had ~40-fold higher inhibitory potency against mutant IDH1 (IC₅₀ = 0.05 μ M vs. 1.7-2.7 μ M for the benzenesulfonamide analogues), as well as more favorable lipophilicity (LogP = 2.2). In accordance with these properties, tissue distribution and preliminary microPET imaging studies revealed good initial uptake and rapid clearance of [¹⁸F]**1** from the normal brain (data not shown), and >95% specific inhibition in IDH1 mutant glioma cells *in vitro*, indicating minimal non-specific binding for [¹⁸F]**1**. The two cell lines used for evaluation of [¹⁸F]**1** in the current study represent clinically relevant models of the most commonly occurring IDH1 (R132H) mutation in glioma. Tissue distribution and microPET imaging were conducted with the genetically engineered IDH1 mutant HOG cell line in view of its ability to form tumors *in vivo*. However, *in vitro* studies with the patient-derived IMA cell line confirmed the ability of [¹⁸F]**1** to bind to the native IDH1-R132H enzyme with high specificity, as blocking with unlabeled **1** decreased the uptake of [¹⁸F]**1** in IMA cells by 90% (**Figure 4A**).

Currently, the standard methods for detection of IDH mutations in gliomas include Sanger sequencing and immunohistochemistry (IHC). The advantages and disadvantages of these techniques have been reviewed in the literature.²² While these methods provide accurate information on mutant IDH1/2 status, they are invasive and generally do not permit monitoring the expression of the mutant IDH enzyme or its activity at the whole tumor level and in longitudinal studies. Over the past several years, a number research groups have investigated the use of proton MRS for measuring D-2-HG levels, as a surrogate marker of IDH1/2 mutations, in gliomas. Although this method has proven to be a valuable tool, it has some limitations, including low sensitivity (requires \geq 1mM D-2-HG for successful detection), low spatial resolution, and potential overlap of the D-2-HG signal in MRS with endogenous brain metabolites such as glutamine (Gln), glutamate (Glu) and N-acetylaspartylglutamate (NAAG).^{10, 23} Furthermore, it has been shown recently that the sensitivity of MRS for detecting D-2-HG in IDH1/2 mutant gliomas is highly dependent on tumor volume.²³ Successful development of PET imaging agents for the mutant IDH1 enzyme can provide a complementary imaging tool to MRS for assessment of IDH1 mutations in glioma. The advantages of PET as an imaging method include high sensitivity in regard to radiolabeled probe detection *in vivo*, good spatial resolution, ability to accurately quantify the radiotracer uptake in the target tissue, and suitability for longitudinal studies.

In conclusion, we have synthesized and evaluated a ¹⁸F-labeled triazinediamine analogue as a potential radiotracer for PET imaging of mutant IDH1 in gliomas. The labeled compound showed high uptake and specific binding in IDH1 mutant glioma cells *in vitro*. Tissue distribution and microPET imaging studies revealed good uptake in IDH1-R132H mutant glioma xenografts, which could be inhibited significantly with excess unlabeled analogue. To the best of our knowledge, these studies represent the first successful demonstration of the feasibility of imaging IDH1 mutations in gliomas by PET.

However, *in vivo* studies with [¹⁸F]**1** also revealed significant bone uptake that increased with time, indicating rapid defluorination of the labeled compound. Therefore, efforts are underway to optimize the chemical structure of [¹⁸F]**1** to increase the metabolic stability, and ideally, its binding affinity and selectivity for mutant IDH1 as well. Future work will include evaluation of analogues of [¹⁸F]**1** in orthotopic mutant IDH1 glioma models to determine the uptake of the labeled inhibitors in tumors vs. the normal brain and to test their ability to image IDH1 mutations by PET.

ASSOCIATED CONTENT

Supporting Information

The Supporting Information is available free of charge on the ACS Publications website.

Materials and methods for chemical syntheses, radiolabeling, *in vitro*- and *in vivo* evaluation of the labeled compound, and % injected dose per gram (%ID/g) data for the biodistribution study.

AUTHOR INFORMATION

Corresponding Author

*E-mail: satish.chitneni@duke.edu.

Author Contributions

The manuscript was written through contributions of all authors. All authors have given approval to the final version of the manuscript.

Funding Sources

This work was supported in part by NIH grant CA182025 and by a research grant from the Pratt School of Engineering at Duke University (Chandran Research Award).

ACKNOWLEDGMENT

We thank Dr. Xiao-Guang Zhao for help with the biodistribution studies, Casey Moure for derivation of the R132H-KO cell line, staff at the Duke Cyclotron facility for production of fluorine-18, and Thomas Hawk and Simone Degan for help with small animal PET/CT imaging studies.

ABBREVIATIONS

IDH, isocitrate dehydrogenase; α -KG, alpha-ketoglutarate; 2-HG, 2-hydroxyglutarate; PET, positron emission tomography; MRS, magnetic resonance spectroscopy; *P*, partition coefficient; HOG, human oligodendroglioma; IC₅₀, half-maximal inhibitory concentration; IMA, IDH1 mutant astrocytoma; WT, wild-type; ID, injected dose; SUV, standardized uptake value; TAC, time-activity curve; KO, knockout.

REFERENCES

- Reitman, Z. J.; Yan, H. Isocitrate Dehydrogenase 1 and 2 Mutations in Cancer: Alterations at a Crossroads of Cellular Metabolism. *J Natl Cancer Inst* **2010**, *102*, *13*, 932-941.
- Yan, H.; Parsons, D. W.; Jin, G. L.; McLendon, R.; Rasheed, B. A.; Yuan, W. S.; Kos, I.; Batinic-Haberle, I.; Jones, S.; Riggins, G. J.; Friedman, H.; Friedman, A.; Reardon, D.; Herndon, J.; Kinzler, K. W.; Velculescu, V. E.; Vogelstein, B.; Bigner, D. D. IDH1 and IDH2 Mutations in Gliomas. *New Engl J Med* **2009**, *360*, *8*, 765-773.
- Dang, L.; White, D. W.; Gross, S.; Bennett, B. D.; Bittinger, M. A.; Driggers, E. M.; Fantin, V. R.; Jang, H. G.; Jin, S.; Keenan, M. C.; Marks, K. M.; Prins, R. M.; Ward, P. S.; Yen, K. E.; Liau, L. M.; Rabinowitz, J. D.; Cantley, L. C.; Thompson, C. B.; Vander Heiden, M. G.; Su, S. M. Cancer-Associated IDH1 Mutations Produce 2-Hydroxyglutarate. *Nature* **2009**, *462*, *7274*, 739-744.

4. Xu, W.; Yang, H.; Liu, Y.; Yang, Y.; Wang, P.; Kim, S.-H.; Ito, S.; Yang, C.; Wang, P.; Xiao, M.-T.; Liu, L.-x.; Jiang, W.-q.; Liu, J.; Zhang, J.-y.; Wang, B.; Frye, S.; Zhang, Y.; Xu, Y.-h.; Lei, Q.-y.; Guan, K.-L.; Zhao, S.-m.; Xiong, Y. Oncometabolite 2-Hydroxyglutarate Is a Competitive Inhibitor of alpha-Ketoglutarate-Dependent Dioxygenases. *Cancer Cell* **2011**, *19*, 1, 17-30.
5. Turcan, S.; Rohle, D.; Goenka, A.; Walsh, L. A.; Fang, F.; Yilmaz, E.; Campos, C.; Fabius, A. W. M.; Lu, C.; Ward, P. S.; Thompson, C. B.; Kaufman, A.; Guryanova, O.; Levine, R.; Heguy, A.; Viale, A.; Morris, L. G. T.; Huse, J. T.; Mellinghoff, I. K.; Chan, T. A. IDH1 Mutation is Sufficient to Establish the Glioma Hypermethylator Phenotype. *Nature* **2012**, *483*, 7390, 479-483.
6. Reitman, Z. J.; Jin, G.; Karoly, E. D.; Spasojevic, I.; Yang, J.; Kinzler, K. W.; He, Y.; Bigner, D. D.; Vogelstein, B.; Yan, H. Profiling the Effects of Isocitrate Dehydrogenase 1 and 2 Mutations on the Cellular Metabolome. *Proc. Natl. Acad. Sci. U.S.A.* **2011**, *108*, 8, 3270-3275.
7. Beiko, J.; Suki, D.; Hess, K. R.; Fox, B. D.; Cheung, V.; Cabral, M.; Shonka, N.; Gilbert, M. R.; Sawaya, R.; Prabhu, S. S.; Weinberg, J.; Lang, F. F.; Aldape, K. D.; Sulman, E. P.; Rao, G.; McCutcheon, I. E.; Cahill, D. P. IDH1 Mutant Malignant Astrocytomas are More Amenable to Surgical Resection and Have a Survival Benefit Associated with Maximal Surgical Resection. *Neuro Oncol* **2014**, *16*, 1, 81-91.
8. Sulkowski, P. L.; Corso, C. D.; Robinson, N. D.; Scanlon, S. E.; Purshouse, K. R.; Bai, H. W.; Liu, Y. F.; Sundaram, R. K.; Hegan, D. C.; Fons, N. R.; Breuer, G. A.; Song, Y. B.; Mishra-Gorur, K.; De Feyter, H. M.; de Graaf, R. A.; Surovtseva, Y. V.; Kachman, M.; Halene, S.; Gunel, M.; Glazer, P. M.; Bindra, R. S. 2-Hydroxyglutarate Produced by Neomorphic IDH Mutations Shomologous Recombination and Induces PARP Inhibitor Sensitivity. *Sci Transl Med* **2017**, *9*, 375, eaal2463.
9. The Cancer Genome Atlas Research Network. Comprehensive, Integrative Genomic Analysis of Diffuse Lower-Grade Gliomas. *N Engl J Med* **2015**, *372*, 26, 2481-2498.
10. Choi, C.; Ganji, S. K.; Deberardinis, R. J.; Hatanpaa, K. J.; Rakheja, D.; Kovacs, Z.; Yang, X. L.; Mashimo, T.; Raisanen, J. M.; Marin-Valencia, I.; Pascual, J. M.; Madden, C. J.; Mickey, B. E.; Malloy, C. M.; Bachoo, R. M.; Maher, E. A., 2-Hydroxyglutarate Detection by Magnetic Resonance Spectroscopy in IDH-Mutated Patients with Gliomas. *Nature Medicine* **2012**, *18*, 4, 624-629.
11. Yen, K.; Travins, J.; Wang, F.; David, M. D.; Artin, E.; Straley, K.; Padyana, A.; Gross, S.; DeLaBarre, B.; Tobin, E.; Chen, Y.; Nagaraja, R.; Choe, S.; Jin, L.; Konteatis, Z.; Cianchetta, G.; Saunders, J. O.; Salituro, F. G.; Quivoron, C.; Opolon, P.; Bawa, O.; Saada, V.; Paci, A.; Broutin, S.; Bernard, O. A.; de Botton, S.; Marteyn, B. S.; Pilichowska, M.; Xu, Y. X.; Fang, C.; Jiang, F.; Wei, W. T.; Jin, S. F.; Silverman, L.; Liu, W.; Yang, H.; Dang, L.; Dorsch, M.; Penard-Lacronique, V.; Biller, S. A.; Su, S. S. M. AG-221, a First-in-Class Therapy Targeting Acute Myeloid Leukemia Harboring Oncogenic IDH2 Mutations. *Cancer Discovery* **2017**, *7*, 5, 478-493.
12. Konteatis, Z. D.; Popovici-Muller, J.; Travins, J. M.; Zahler, R.; Cai, Z.; Zhou, D. Therapeutically Active Compounds and Their Methods of Use. Patent WO 2015/003640 A1.
13. Chitneni, S. K.; Deroose, C. M.; Balzarini, J.; Gijssbers, R.; Celen, S.; Debyser, Z.; Mortelmans, L.; Verbruggen, A. M.; Bormans, G. M. A *p*-[¹⁸F]Fluoroethoxyphenyl Bicyclic Nucleoside Analogue as a Potential Positron Emission Tomography Imaging Agent for Varicella-Zoster Virus Thymidine Kinase Gene Expression. *J Med Chem* **2007**, *50*, 26, 6627-6637.
14. Popovici-Muller, J.; Saunders, J. O.; Salituro, F. G.; Travins, J. M.; Yan, S.; Zhao, F.; Gross, S.; Dang, L.; Yen, K. E.; Yang, H.; Straley, K. S.; Jin, S.; Kunii, K.; Fantin, V. R.; Zhang, S.; Pan, Q.; Shi, D.; Biller, S. A.; Su, S. M. Discovery of the First Potent Inhibitors of Mutant IDH1 That Lower Tumor 2-HG In Vivo. *ACS Med Chem Lett* **2012**, *3*, 10, 850-855.
15. Okoye-Okafor, U. C.; Bartholdy, B.; Cartier, J.; Gao, E. N.; Pietrak, B.; Rendina, A. R.; Rominger, C.; Quinn, C.; Smallwood, A.; Wiggall, K. J.; Reif, A. J.; Schmidt, S. J.; Qi, H. W.; Zhao, H. Z.; Joberty, G.; Faelth-Savitski, M.; Bantscheff, M.; Drewes, G.; Duraiswami, C.; Brady, P.; Groy, A.; Narayanagari, S. R.; Antony-Debre, I.; Mitchell, K.; Wang, H. R.; Kao, Y. R.; Christopheit, M.; Carvajal, L.; Barreyro, L.; Paietta, E.; Makishima, H.; Will, B.; Concha, N.; Adams, N. D.; Schwartz, B.; McCabe, M. T.; Maciejewski, J.; Verma, A.; Steidl, U. New IDH1 Mutant Inhibitors for Treatment of Acute Myeloid Leukemia. *Nat Chem Biol* **2015**, *11*, 11, 878-886.
16. Jin, G.; Reitman, Z. J.; Duncan, C. G.; Spasojevic, I.; Gooden, D. M.; Rasheed, B. A.; Yang, R.; Lopez, G. Y.; He, Y.; McLendon, R. E.; Bigner, D. D.; Yan, H. Disruption of Wild-Type IDH1 Suppresses D-2-Hydroxyglutarate Production in IDH1-Mutated Gliomas. *Cancer Res* **2013**, *73*, 2, 496-501.
17. Eckelman, W. C.; Kilbourn, M. R.; Mathis, C. A., Discussion of Targeting Proteins In Vivo: In Vitro Guidelines. *Nucl Med Biol* **2006**, *33*, 4, 449-451.
18. Tallman, M. S.; Knight, R. D.; Glasmacher, A. G.; Dohner, H. Phase III Randomized, Ppen-Label Study Comparing the Efficacy and Safety of AG-221 vs Conventional Care Regimens (CCR) in Older Patients With Advanced Acute Myeloid Leukemia (AML) With Isocitrate Dehydrogenase (IDH)-2 Mutations in Relapse or Refractory to Multiple Prior Treatments: The IDHENTIFY Trial. *J. Clin. Oncol.* **2016**, *34*, 15 suppl.
19. Davis, M. I.; Gross, S.; Shen, M.; Straley, K. S.; Pragani, R.; Lea, W. A.; Popovici-Muller, J.; DeLaBarre, B.; Artin, E.; Thorne, N.; Auld, D. S.; Li, Z.; Dang, L.; Boxer, M. B.; Simeonov, A. Biochemical, Cellular, and Biophysical Characterization of a Potent Inhibitor of Mutant Isocitrate Dehydrogenase IDH1. *J Biol Chem* **2014**, *289*, 20, 13717-13725.
20. Deng, G.; Shen, J.; Yin, M.; McManus, J.; Mathieu, M.; Gee, P.; He, T.; Shi, C.; Bedel, O.; McLean, L. R.; Le-Strat, F.; Zhang, Y.; Marquette, J. P.; Gao, Q.; Zhang, B.; Rak, A.; Hoffmann, D.; Rooney, E.; Vassort, A.; Englaro, W.; Li, Y.; Patel, V.; Adrian, F.; Gross, S.; Wiederschain, D.; Cheng, H.; Licht, S. Selective Inhibition of Mutant Isocitrate Dehydrogenase 1 (IDH1) via Disruption of a Metal Binding Network by an Allosteric Small Molecule. *J Biol Chem* **2015**, *290*, 2, 762-774.
21. Chitneni, S. K.; Reitman, Z. J.; Gooden, D. M.; Yan, H.; Zalutsky, M. R. Radiolabeled Inhibitors as Probes for Imaging Mutant IDH1 Expression in Gliomas: Synthesis and Preliminary Evaluation of Labeled Butyl-Phenyl Sulfonamide Analogs. *Eur J Med Chem* **2016**, *119*, 218-230.
22. Arita, H.; Narita, Y.; Yoshida, A.; Hashimoto, N.; Yoshimine, T.; Ichimura, K. IDH1/2 Mutation Detection in Gliomas. *Brain Tumor Pathol* **2015**, *32*, 2, 79-89.
23. de la Fuente, M. I.; Young, R. J.; Rubel, J.; Rosenblum, M.; Tisnado, J.; Briggs, S.; Arevalo-Perez, J.; Cross, J. R.; Campos, C.; Straley, K.; Zhu, D.; Dong, C.; Thomas, A.; Omuro, A. A.; Nolan, C. P.; Pentsova, E.; Kaley, T. J.; Oh, J. H.; Noeske, R.; Maher, E.; Choi, C.; Gutin, P. H.; Holodny, A. I.; Yen, K.; DeAngelis, L. M.; Mellinghoff, I. K.; Thakur, S. B. Integration of 2-Hydroxyglutarate-Proton Magnetic Resonance Spectroscopy into Clinical Practice for Disease Monitoring in Isocitrate Dehydrogenase-Mutant Glioma. *Neuro Oncol* **2016**, *18*, 2, 283-290.

Table of Contents artwork

